HOSTED BY

ELSEVIER

Contents lists available at ScienceDirect

Saudi Journal of Biological Sciences

journal homepage: www.sciencedirect.com

الجمعية السعودية لعلوم الحياة
SAUDI BIOLOGICAL SOCIETY

Original article

Designing of fragment based inhibitors with improved activity against *E. coli* AmpC β-lactamase compared to the conventional antibiotics

Sidrah Hafeez [a], Rehan Zafar Paracha [b], Fazal Adnan [a,*]

[a] *Atta-ur-Rahman School of Applied Biosciences (ASAB), National University of Sciences and Technology (NUST), Islamabad 44000, Pakistan*
[b] *School of Interdisciplinary Engineering and Sciences (SINES), National University of Science and Technology (NUST), Islamabad 44000, Pakistan*

ARTICLE INFO

Keywords:
Multi drug resistance
UTIs
AmpC β-lactamase
Fragment based drug design
Cefepime
Molecular dynamic simulations

ABSTRACT

One of the most common primary resistance mechanism of multi-drug resistant (MDR) Gram negative pathogenic bacteria to combat β-lactam antibiotics, such as penicillins, cephalosporins and carbapenems is the generation of β- lactamases. The uropathogenic *E. coli* is mostly getting multi-drug resistance due to the synthesis of AmpC β-lactamases and therefore new antibiotics and inhibitors are needed to treat the evolving infections. The current study was designed for targetting AmpC β-lactamase of *E. coli* using molecular docking based virtual screening, linking fragments for designing novel compounds and binding mode analysis using molecular dynamic simulation with target protein. The FCH group all-purpose fragment library consisting of 9388 fragments has been screened against AmpC β-lactamase protein of *E. coli* and the antibiotics and anti-infectives used in treatment of Urinary tract Infections (UTIs) were also screened with AmpC β-lactamase protein. Among the 9388 fragments, 339 fragment candidates were selected and linked with cefepime antibiotic having maximum binding affinity for AmpC target protein. Computational analysis of interactions as well as molecular dynamics (MD) simulations were also conducted for identifying the most promising ligand-pocket complexes from docking investigations to comprehend their thermodynamic properties and verify the docking outcomes as well. Overall, the linked complexes (LCs) showed good binding interactions with AmpC β-lactamase. Interestingly, our fragment-based LCs remained relatively stable in comparison with cefepime antibiotic. Moreover, S12 fragment linked complex remained the most stable during 50 ns with remarkable number of interactions indicating it as promising candidate in novel lead discovery against MDR *E. coli* infections.

1. Introduction

Antimicrobial resistance is one of the ten major global health burdens that is continuously increasing the rate of mortality and morbidity associated with bacterial infections. The overall economic cost of AMR because of resistance in the clinically important pathogens including *Staphylococcus aureus*, *Escherichia coli*, *Klebsiella pneumoniae*, *Acinetobacter baumanii*, *Pseudomonas aeruginosa* and *Enterococcus faecium* was reported to be $2.9 billion in the US alone (León-Buitimea et al., 2021, Friedman et al., 2016, Shrestha et al., 2018). *E. coli* is a commensal as well as an opportunistic pathogen that is resident in the mammalian digestive tract. Additionally, *E. coli* is the etiological agent behind many extra-intestinal infections (ExPEC), such as the urinary tract infections (UTIs) (Haenni et al., 2014, Pitout, 2012).

UTIs are one of the most prevalent infectious diseases in humans representing about 40 % of all nosocomial infections and 50 % of all bacterial infections associated with increased morbidity (Karam et al., 2019). UTIs are also an important economic concern due to the significant financial burden on healthcare system. In the United States, about 11 million people receive treatment for UTIs each year at a cost of about $6 billion (Mann et al., 2017). UTIs are caused by different pathogens, but most commonly by *E. coli*, *K. pneumoniae*, *Proteus mirabilis*, *Enterococcus faecalis* and *Staphylococcus saprophyticus*. Among all the causes, the most frequent etiological factor of UTIs both complicated and uncomplicated is uropathogenic *Escherichia coli* (UPEC) (Rezatofighi et al., 2021, Bischoff et al., 2018). UPEC has been reported to be the main cause of upto 95 % of uncomplicated and 50 % of complicated UTI cases (Tan and Chlebicki, 2016).

β-Lactam antibiotics hold a place as central antimicrobials for the treatment of bacterial infections due to their broad activity spectrum, clinical effectiveness and good safety profile (Spyrakis et al., 2020, Lima et al., 2020). The antibiotics such β-lactams, trimethoprim,

* Corresponding author.
E-mail address: adnanfazal@asab.nust.edu.pk (F. Adnan).

https://doi.org/10.1016/j.sjbs.2023.103884
Received 24 March 2023; Received in revised form 19 November 2023; Accepted 24 November 2023
Available online 25 November 2023

nitrofurantoin, and quinolones are frequently used as routine UTI treatment in many different countries. The extensive utilization of these antibacterials is the reason behind alarming levels of combined drug resistance against third generation and higher cephalosporins, aminoglycoside and floroquinolone drug classes in case of pathogens like *Escherichia coli* and *Klebsiella pneumoniae* (Weiner et al., 2016). It is predicted that *E. coli* would develop resistance to every known antibiotic by 2050, transforming into incurable superbugs (O'Neill, 2014). Therefore, comprehension of the impact of drug resistance along with the development of novel strategies is of prime importance (Ghosh and Mukherjee, 2016, Gales et al., 2000).

Gram negative bacteria especially *E. coli* produce AmpC β-lactamase as one of the most common causes of resistance to β-lactam antibiotics. These AmpC β-lactamases cause resistance against different derivatives of penicillins, certain broad and extended spectrum cephalosporins and monobactams (Jacoby, 2009). These AmpC β-lactamases are also resistant to β-lactamase inhibitors like clavulanic acid (Ejaz et al., 2014). The secretion of β-lactamases hydrolytic enzymes have gained significant importance as resistance mechanism opted by various bacteria to hydrolyse β-lactam antibiotics (Fisher et al., 2005).

AmpC β-lactamases develop when the chromosomal AmpC gene is overexpressed or when a plasmid-mediated AmpC determinant is acquired (Pfeifer et al., 2010). Plasmid-mediated AmpC (pAmpC) genes were reported for the first time in 1988 (Swaminathan et al., 2001). Although pAmpC β-lactamases occur worldwide but they have been less explored in *E. coli*. These enzymes have narrowed down therapeutic options as they have been typically associated with multiple antibiotic resistances (Black et al., 2005). AmpC β-lactamases in *E. coli* are less explored as compared to these enzymes in other genera of Enterobacteriaceae family, but the constitutive over-expression of chromosomal ampC gene is being reported largely in many clinical isolates (Haenni et al., 2014). Therefore we have considered AmpC β-lactamase protein of *E. coli* in our work.

During the past 25 years, the fragment-based drug design (FBDD) has proven to be a very effective and alternative approach to high-throughput screening (HTS) in identification of quality leads as clinical candidates and approved medicines. FBDD campaigns have succeeded in establishing their place in medicinal chemistry, biotechnology and pharmaceutical sciences along with academic research by discovery of four fragment based drugs available in the market and more than 40 in clinical trials (Konteatis, 2021, Erlanson et al., 2016, Nichols et al., 2014). FBDD is an effective approach for the development of potent compounds from the fragments. In FBDD, a compound is often generated from a simple low affinity chemical fragment with less chemical complexity, and low molecular weight (less than 300 Da)(Li, 2020). Vemurafenib (Bollag et al., 2010) was the first drug originated from a fragment screening, that was approved in 2011 by the Food and Drug Administration (FDA). Similarly, two other drugs venetoclax (Li, 2020) and erdafitinib (Murray et al., 2019) were approved in 2016 and 2019, respectively. Vemurafenib and erdafitinib are the examples of drugs developed by fragment growing approach, whereas venetoclax was produced as a result of the fragment linking method.

The present study has been designed considering the importance of fragment based drug design. In this study, we have screened fragment database with AmpC β-lactamase protein and linked best affinity antibiotic with best fragments, their interactions were computed as well as their molecular dynamic simulations have been carried out to find out potential candidates against AmpC β-lactamase target protein. Moreover, two potential fragments in linked complexes were linked together that exhibited best activity among all complexes and can help in the future to design more potent AmpC β-lactamase inhibitors.

2. Materials & methods

The overall scheme of methodology is represented in (Fig. 1).

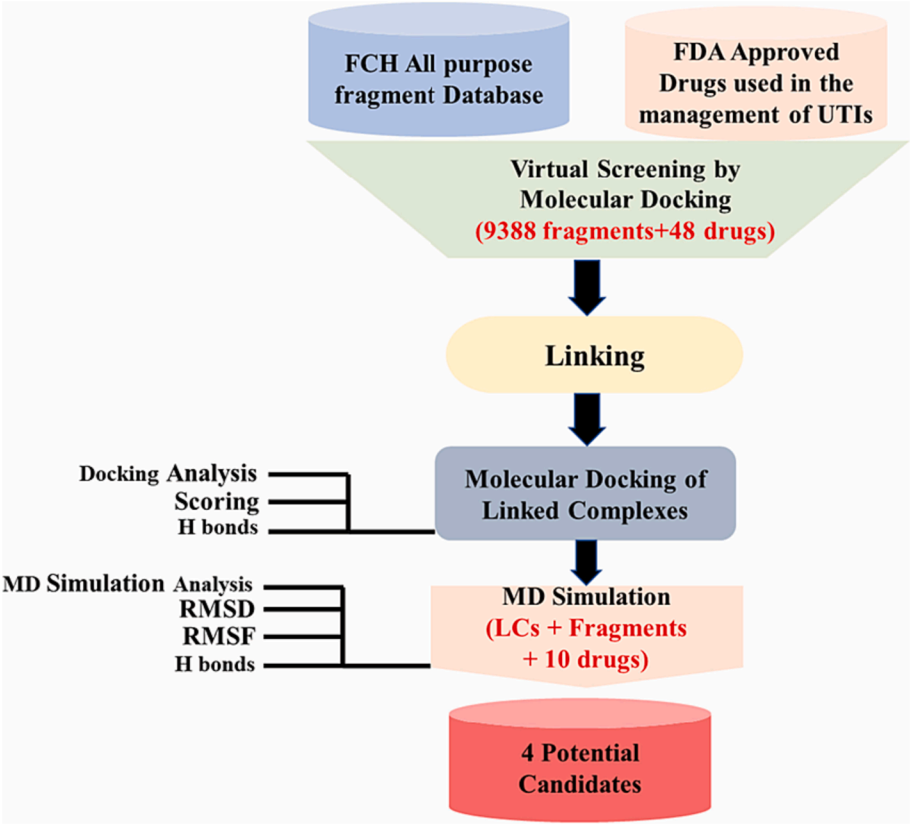

Fig. 1. Schematic diagram showing step-wise methodology of the study conducted.

2.1. Fragment library

To begin the process of fragment based screening, small compounds called"fragments" are required as starting point (Chilingaryan et al., 2018, Chilingaryan et al., 2012). All-purpose fragment library was obtained from FCH group (http://fchgroup.net/fragment-libraries.php) that consisted of 9388 fragments. This fragment library was selected in this study as it consisted of fragments with versatile functional groups and has not been tested against AmpC β-lactamases. Moreover, FCH group claims that this library has been used for lead discovery with its two drugs approved and thirty of these fragments are in clinical trials. FCH group fragment libraries have been used in fragment tailoring strategies for novel chemical entities against novel corona virus as well (Choudhury, 2021). Fragment database was subjected to protonation. In the next step, partial charges were calculated and applied to the fragments. Energy minimization with a MMFF94 forcefield was then performed for proper molecular arrangement within the space.

2.2. AmpC β-lactamase protein structure retrieval and preparation for docking

The crystal structure of AmpC β-lactamase of *E. coli* was downloaded from RCSB Protein Databank (RCSB-PDB) (https://www.rscb.org) (PDB Id 3BLS) with good resolution of 2.30 Å. The protein structure is then prepared by PlayMolecule TM (http://www.playmolecule.org) (Martínez-Rosell et al., 2017) where the protein is protonated at 7.4 pH and its H bond networks were optimized into their standard geometry. The structure was also refined by structure preparation wizard of MOE for corrections of all the issues in protein structure. In this process, removal of all solvent molecules was performed and energy was minimized. The active site was identified by Site Finder followed by dummy atoms creation from the resulting alpha spheres. This prepared protein structure was further used for downstream analysis.

2.3. Prediction and validation of active site of target protein

The prepared protein was subjected to DogSiteScorer (https://bio.tools/dogsitescorer) for binding site prediction and druggability assessment. This server was used for validation of active site residues (Volkamer et al., 2012). The active residues in the catalytic site for ligand attachment are determined by binding site prediction.

2.4. Molecular docking of the fragments with AmpC β-lactamase protein

To find a potential fragment-based candidate against AmpC β –lactamase of *E. coli*, molecular docking studies were performed. Molecular docking simulations were carried out by using MOE Dock function of Molecular Operating Environment (MOE) 2015.10. All already prepared fragments were then dockedm at dummy atoms created at active site of the protein. For performing docking analysis, triangle matcher and refinement approaches were employed. The rigid receptor refinement methodology and GBVI/WSA dG was used. The best 05 poses were selected from 10 different poses for each tested fragment. The scoring methods were set to their default values (Samra et al., 2021). The lowest energy-minimized poses were used for further analysis. On the basis of the S score, interactions between inhibitors and receptor proteins were predicted (Vilar et al., 2008).

2.5. Molecular docking of antibiotics used for urinary tract infections (UTI) with AmpC β-lactamase protein

A total of 48 antibiotics and anti-infectives used for treatment of UTI were selected and their structures were retrieved and downloaded from drug bank https://go.drugbank.com/. The structures of antibiotics are depicted in (Figure. S1). These antibiotic structures were then imported in MOE and prepared and docked in the binding pocket of AmpC β-lactamase protein. The docked protein-antibiotic complex with maximum binding affinity was selected for further downstream analysis. Cefepime complex was visualized along with all the docked protein-fragment complexes for linking purpose.

2.6. Protein ligand interaction fingerprinting

Protein-Ligand Interaction fingerprinting (PLIF) is a powerful tool for analysis and accurate evaluation of the resultant docking poses for identifying the most suitable binding mode for each molecule and generating a relative ranking of different molecules. Protein-Ligand Interaction fingerprinting analysis was run for all docked complexes to explicate the frequency of protein ligand interactions within binding site using MOE v 2015.10. PLIF analysis is a graphical demonstration of the frequency of each interacting residue in all ligands-protein complexes or the occurrence frequency of each fingerprint bit. The PLIF interactions are depicted by HBD (side chain hydrogen bond donor), HBA (side chain hydrogen bond acceptor), HBd (hydrogen bond donor of backbone), Hba (hydrogen bond acceptor of backbone) and also arene interactions.

2.7. Linking fragments with cefepime and their screening

The selected fragments were visualized with antibiotic in pymol 2.4.1 and all superimposed complexes were selected. All the selected fragments were imported to ACD Chemsketch Freeware version 2020.1.2 and linked to cefepime resulting in the formation of stable antibiotic-fragment complex formation. All rules of chemical bond formation were considered in formation of complexes. The linked drug complexes were screened with AmpC β-lactamase in order to determine the new drug complex conformations and orientation within active site along with the determination of the binding affinity.

2.8. Linking of best fragments (S12) and their molecular docking

Fragment linking is one method of generating potent inhibitor compounds using different fragments. In this method, a novel lead molecule can be created by linkage of two or more fragments together (Yu et al., 2020). The binding affinities can be significantly improved by using this technique (Mondal et al., 2016). The top fragments that appeared in linked cefepime drug complexes with promising docking scores i.e. f-1 (f_2_3871) and f-2 (f_2_78) were linked together to form new fragment complex S12. S12 was then screened for the active site of AmpC β-lactamase for assessing its binding affinity with target protein as well as for its comparison with LCs.

2.9. Molecular dynamics simulations of promising inhibitors

The molecular dynamics simulation analysis is extensively utilized in drug discovery for investigating protein–ligand complexes at atomic level (Hollingsworth and Dror, 2018). The most promising leads and best affinity antibiotics (Table.1) in complex with AmpC protein were selected for 50 ns molecular dynamics simulation using a GROMACS 5.1

Table 1
MD Simulation studies of Antibiotics.

Sr. No.	Antibiotics	DB accession number	Docking Score (kcal/mol)
1.	Cefepime	DB01413	−11.65
2.	Cefotetan	DB01330	−9.45
3.	Cefoperazone	DB01329	−9.41
4.	Ceftolozane	DB09050	−9.29
5.	Ceftriaxone	DB01212	−9.27
6.	Cefiderocol	DB14879	−8.86
7.	Piperacillin	DB00319	−8.63
8.	Aztreonam	DB00355	−8.45
9.	Ceftazidime	DB00438	−8.32
10.	Meropenem	DB00760	−8.14

software package (GNU, General Public License; http://www.gromacs.org). The CHARMM36 force field was used (da Silva et al., 2022). The selected ligand–protein complex was firstly solvated within a cubic box with a three-points (TIP3P) water model (100 × 100 × 100 A) (Izadi et al., 2014). The CHARMM force field parameters for each ligand were generated using CHARMM General Force Field (CGenFF) program (ParamChem project; https://cgenff.umaryland.edu/) (Vanommeslaeghe et al., 2010). All of the complexes were then simulated within a cubic box at 1 Å of buffer distance. During this process, electroneutralization of the complexes was maintained using respective number of ions added via Monte-Carlo ion-placing method (Ross et al., 2018). The steepest decent minimization algorithm was used for neutralization of the system energy. After the energy minimization, all of these complexes were subjected firstly to 100 ps of NVT equilibration and then 100 ps of NPT equilibration. Final molecular dynamics simulation was performed for 50 ns. Different analysis modules from the GROMACS package were used to conduct structural and conformational analysis. After completion, root mean square deviations (RMSD), the root mean square fluctuations (RMSF), and the hydrogen bonds were calculated between the protein and the ligands by using GROMACS analysis tools and also visualized via Visual Molecular Dynamics 1.9.3 (VMD) package (Humphrey et al., 1996).

3. Results

3.1. Validation of binding pocket of protein

The active site of AmpC β-lactamase (3BLS) active site was predicted by DogsiteScorer (Table. S1). Total nine pockets were predicted and pockets with maximum drug score included Pocket one (P_0) and pocket two (P_1) with drug score of 0.78 and 0.87, respectively. The pocket P_0 contains the residues Gly63, Ser64, Lys67, Thr111, Leu119, Gln120, Arg148, Asn152, Val211, Tyr221, Trp260, Gln 261, Tyr266, Glu272, Leu274, Ser282,Gly286, Ile291, Arg296, Val298, His 314,Thr316, Tyr325, Asn 343, Asn346, Arg349 that have been verified by SiteFinder of MOE suite (Table. S2). Also, another previous study reports Ser64 as essential catalytic residue of AmpC, that acetylates during the hydrolysis of β-lactam ring. Similarly, Lys67, Gln120, Tyr150, Asn152, Lys315, Thr316 and Ala318 are other important active-site residues that were involved in binding (Usher et al., 1998). After validation of P_0 residues, it was used for downstream analysis.

3.2. Molecular docking of the fragments with AmpC β-lactamase protein

The molecular docking simulations were carried out for investigating the potentiality of fragments against AmpC β- lactamase protein active site. Fragment database comprised of 9388 fragments was screened for AmpC β-lactamase protein active site. Out of these fragments, the fragments with least values of binding affinities were selected. The most negative energies represent the best scored fragment. Among all of the fragments, 339 best fragments were obtained with a minimum energy score of −7.69 kcal/mol and a maximum score of −7.0 kcal/mol.

3.3. Molecular docking of antibiotics used for UTI with AmpC β-lactamase protein

Molecular docking studies were also performed for 48 antibiotics and antiinfectives commonly used as treatment regimen for urinary tract infections using MOE 2015.10 suite. Out of these antibiotics, Cefepime has the maximum binding affinity for AmpC β-lactamase protein with score of −11.65 kcal/mol, whereas, Methenamine possessed the lowest affinity with a value of 0.01 kcal/mol (Table.2).

The docking scores of all the studied drugs are presented in the form of boxplot (Fig. 2). According to the boxplot, cefepime has the median score of −7.5 and the lowest score of −11.65. Comparatively, one of the poses of cefepime possessing the better binding affinity value of −11.6 kcal/mol was selected and its interactions and other binding poses were computed. The residues that participated in interactions include Asn289, Asn 346, Ser64, Gly317, Ala318, Asn152 and Lys315. It showed H bonding with Asn152, Ser212, Asn289, Gly320, Gly321, Asn346 and Arg349 whereas hydrophobic interactions were formed with Asn289, Leu293 and Ala318. This binding affinity value as well as good interaction pattern of cefepime makes it a good candidate for linking with fragments. Other antibiotics showing binding affinities next to cefepime include cefotetan with a score of −9.45 kcal/mol and cefoperazone with affinity value of −9.41 kcal/mol.

Table 2
Computed Binding Affinities of Antibiotics against AmpC β-lactamase protein.

Drugs	Binding Affinities (Kcal/mol)	Drugs	Binding Affinities (Kcal/mol)
Cefepime	−11.65	Ciprofloxacin	−7.00
Cefotetan	−9.45	Amoxicillin	−6.79
Cefoperazone	−9.41	Imipenem	−6.78
Ceftolozane	−9.29	Vaborbactam	−6.76
Ceftriaxone	−9.27	Cefoxitin	−6.62
Cefiderocol	−8.86	Cefaclor	−6.55
Piperacillin	−8.63	Relebactam	−6.35
Aztreonam	−8.45	Trimethoprim	−6.34
Ceftazidime	−8.32	Cefadroxil	−6.28
Meropenem	−8.14	Sulfamethoxazole	−6.10
Cefazolin	−8.01	Avibactam	−6.09
Cefotaxime	−7.71	Ampicillin	−6.01
Cefixime	−7.67	Amikacin	−5.86
Cefpodoxime	−7.65	Cefalexin	−5.71
Norfloxacin	−7.59	Nitrofurantoin	−5.65
Cilastatin	−7.52	Phenyl salicylate	−5.51
Pivmecillinam	−7.49	Tazobactam	−5.49
Hyoscyamine	−7.36	Clavulanic acid	−5.26
Ertapenem	−7.31	Gentamicin	−5.08
Doxycycline	−7.14	Sulbactam	−4.91
Ofloxacin	−7.07	Benzoic acid	−4.63
Plazomicin	−7.05	Fosfomycin	−4.58
Levofloxacin	−7.04	Acetohydroxamic acid	−3.99
Cefuroxime	−7.04	Methenamine	−2.78

Cefepime is fourth generation cephalosporin. The structural analysis suggests that β-lactam ring is required for PBP reactivity and antibacterial activity (Vaidya and Jain, 2017). This has been considered while linking of fragments with cefepime to form newer drug complexes. The β-lactam ring of Cefepime is forming hydrogen bond with Ser64 of target protein as well as additional hydrogen bonds are formed with Asn346, Asn289, Gly317, Ala318 and Asn152 of AmpC β-lactamase of *E. coli* (Figure. S2).

3.4. Protein ligand interaction fingerprinting

Protein ligand interaction fingerprinting was performed for the best 339 fragments having maximum binding affinity and results of 332 fragments were obtained. The interaction analysis of the top fragment poses with good binding affinities has been depicted in (Figure.S3). It indicated that Glu272 is the most commonly occurring interaction. Other interactions occurring in these 339 fragments include Lys315, Thr316, Met265, and Arg148, Gly286, Ser64, Asn346, and Tyr150. Thus, Glu272, Lys315, Thr316, Met265, and Arg148 contribute to be the most important residues of active site.

3.5. Linking fragments with cefepime

All fragments having best affinity score were linked with Cefepime for generation of linked complexes. As a result, one hundred and nineteen new linked complexes (LC1 to LC119) were formed. Structures of these LCs are mentioned in (Table. S3).

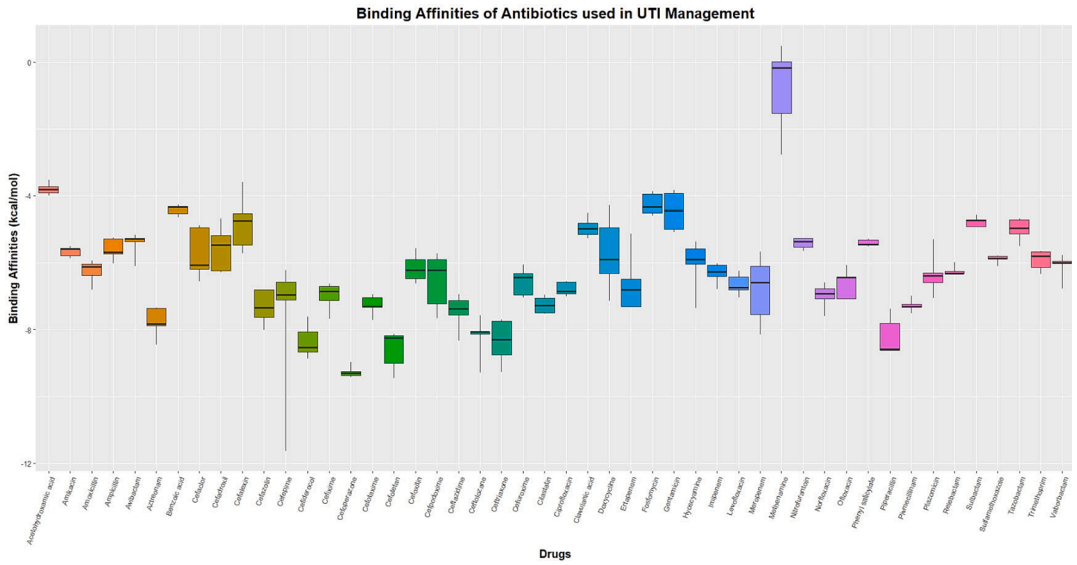

Fig. 2. Boxplot of docking score of antibiotics used in the management of UTI caused by UPEC. The Y-axis represents the affinity scores while X-axis represents the name of the antibiotics. Antibiotics show differential binding affinity pattern against the target protein.

3.6. Molecular docking based screening of linked complexes with AmpC β-lactamase

All of the 119 linked antibiotic-fragment complexes (LCs) were screened for the active site of AmpC β-lactamase protein using same docking parameters as used for antibiotics and fragments docking. As a result, three complexes showed promising docking scores, named as LC-1, LC-2 and LC-3. LC-1 showed maximum affinity with score of −9.54 kcal/mol, LC-2 had 2 poses that possessed maximum docking score of −9.19 and −9.16 kcal/mol respectively. LC-3 exhibited binding affinity of −9.13 kcal/mol. Although these LCs exhibit less binding affinity values than cefepime alone but these affinity values are higher than binding affinity scores of all these separate fragments. The chemical structures of all linked complexes are illustrated in the (Fig. 3).

3.7. Protein ligand interaction of linked complexes

Top three lead compounds having docking scores of −9.54, −9.19 and −9.13 kcal/mol were selected and their protein interactions were computed which illustrated that Ser212 amino acid is interacting with all of the lead compounds. Moreover, sulfur present in LC-2 is interacting with Gln120 and oxygen of LC-3 is interacting Asn289 in the target protein. Furthermore, it was also revealed that the protein ligand interaction pattern of these three top linked complexes showed increased contact points with protein after 50 ns of MD simulation. The interactions of LC-1 include hydrogen bonding with Ser212 and Val211. The interactions with protein increased during the course of 50 ns MD simulations. These interactions include hydrogen bonding with Glu61, Tyr221, Gly320 and Arg204. Moreover, LC-1 is also forming four ionic bonds with Arg204 residue (Figure. S4). LC-2 forms hydrogen bonds

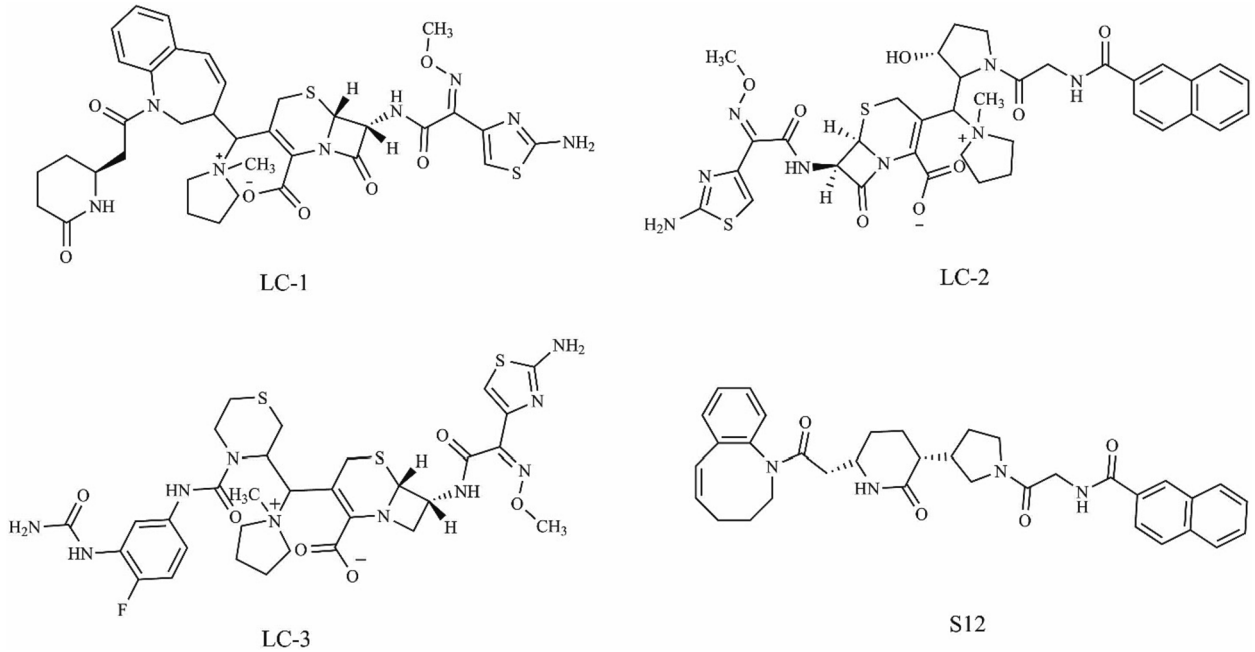

Fig. 3. Chemical structures of best affinity Linked complexes (LCs).

with Gln120 and Ser212 (Figure. S5). The interactions of this complex also increased during 50 ns MD simulation studies. It includes interactions with Arg204, Gly320 and His210 residues. LC-3 interacts with Asn289 and Ser212 whereas it formed two hydrogen bonds with Asp123 residue during 50 ns simulation studies (Figure. S6).

In comparison to LCs, the fragment f1 having score −7.14 kcal/mol showed hydrogen bonding interactions with Arg148 whereas f2 showing binding affinity value of −7.13 kcal/mol formed interactions with Lys315 and f3 fragment with binding affinity value of −7.16 kcal/mol depicted hydrogen bond interactions with Lys315, Thr316 and Asn289. The binding interactions of the fragments are represented in (Figure. S7).

3.8. Linking of fragments f1 with f2 (S12) and their molecular docking analysis

The fragments that appeared in LCs with promising docking scores were further linked together to form new fragment complex (S12) and were then docked in the active site of AmpC β-lactamase showing good binding affinity with score of −9.88 kcal/mol. The fragment complex exhibited good interactions with the target protein (Fig. 4). Major interactions include hydrogen bonding with Ser64, Arg148, Tyr150, Lys315, Thr316, Ala318 and hydrophobic interactions with Leu119, Thr262, Met265, Ile291, Ala292 and Arg296. S12 showed good number of interactions which include two hydrogen bonds with Arg148, two hydrogen bond interactions with Ser64 and one interaction with Ala318 after 50 ns MD simulation. The increased number of interactions show increased adaptability of complex within the binding pocket.

3.9. Molecular dynamics simulation analysis of promising inhibitors

The MD simulation studies are carried out to study the dynamics of ligand-target complexes and determination of their relative stability. Also, MD simulations provide more clear insight of the complex conformation space in comparison to the static image depicted by molecular docking alone (Karplus and Petsko, 1990). The top docked ligands, with promising affinity as well as cefepime and antibiotics were subjected to 50 ns of MD simulation for the assessment of conformational changes of the drug/target complexes during this period. The structural stability of the designed compounds were evaluated through the RMSD and RMSF values of the given protein–ligand complex (Wedberg et al., 2012).

3.9.1. Root mean square deviation

The newly designed linked complexes remained stable during 50 ns MD simulation studies. LC-1 showed fluctuation of 0.8 nm and remained within the acceptable range throughout the course of MD simulations. LC-2 showed relatively stable configuration after 15 ns and remained stabilized till the end. LC-3 remained stable till 35 ns and then fluctuated between 1 and 1.5 nm but remained stabilized till the end. Interestingly, among all the fragment based complexes S12 remained the most stable by showing negligible fluctuations in RMSD values. The RMSD plot of all linked complexes in comparison to cefepime are shown in (Fig. 5A). Moreover, the number of interactions of protein with the LCs improved alot during the course of 50 ns simulations as listed in (Table.S4).

MD simulation was also performed on fragments that were used in formation of linked complexes and their results were presented in a graph (Fig. 5B). f1 and f3 fragments showed fluctuation of only 0.25 nm and remained stable throughout 50 ns simulations. f2 fragment remained completely stable for 30 ns and fluctuated 0.2 nm during period of 40 to 50 nm.

Subsequently, the top ten antibiotics with the best binding affinity were subjected to molecular dynamic simulation for 50 ns to check the flexibility as well as stability of all the docked complexes. The RMSD for the protein backbone C-α atoms in complex with antibiotics were calculated and represented by graph depicted in (Fig. 5C). The best affinity Cefepime showed various fluctuations in RMSD values at 10–20 ns to 6 nm and then the complex got stabilized between 25 and 45 ns at RMSD value of 3.5–4.5 nm after that it showed fluctuation of 2 nm in root mean square deviation values. It was also observed that it was removed from the trajectory. Cefotetan remains unstable and its plot of trajectory shows initial fluctuation of 0.3 nm till 10 ns and jumps to higher magnitude after 20 ns and remained fluctuating til 0.8 nm. Cefoperazone shows fluctuations in the range starting from 0.2 nm to 0.45 nm. The RMSD plot of Ceftolozane shows that it keeps on fluctuating between 0.3 and 0.9 nm throughout 50 ns. Ceftriaxone shows a stable behavior it starts fluctuations from 0.4 nm but comes to 0.3 nm and remains stable till the end. Cefiderocol shows the range of 0.45 nm initially and fluctuates till 1.25 nm at 25 ns but then shows a stable trajectory at 0.75 nm with minor fluctuations till 50 ns. Piperacillin shows relatively stable trajectory with initial minor fluctuations of 0.3 to 0.4 nm at 10 ns and stabilizes after 20 ns between 0.4 and 0.5 nm till 50 ns. Comparatively, Aztreonam showed the most stable trajectory showing fluctuation of 0.2 nm to 0.3 nm till 40 ns and remained stable from 40 to 50 ns. Ceftazidime fluctuates in the range of 0.3 to 0.4 ns for 5 ns and after 10 ns, it shows fluctuations between 0.45 nm and 0.6 nm. Lastly, Meropenem RMSD plot shows initial fluctuations of 0.5 nm to 0.75 nm up-to 5 ns and then stabilizes at 0.85 nm with small peaks throughout 50 ns. Overall, antibiotics showed stable trajectories in comparison to cefepime.

3.9.2. Root mean square fluctuation

The root-mean-square fluctuation (RMSF) plot computes the average deviation of a protein residue over a period of time from one reference position that generally occurs upon ligand interaction. Thus, RMSF plot is an indication of portions that are fluctuating from their mean structure. The low RMSF values show that structure is compact and the high RMSF values correspond to flexibility due to loop regions that in turn indicate increased interaction potential with the ligand molecule. The RMSF plot of 50 ns simulation trajectories of LCs bound protein is

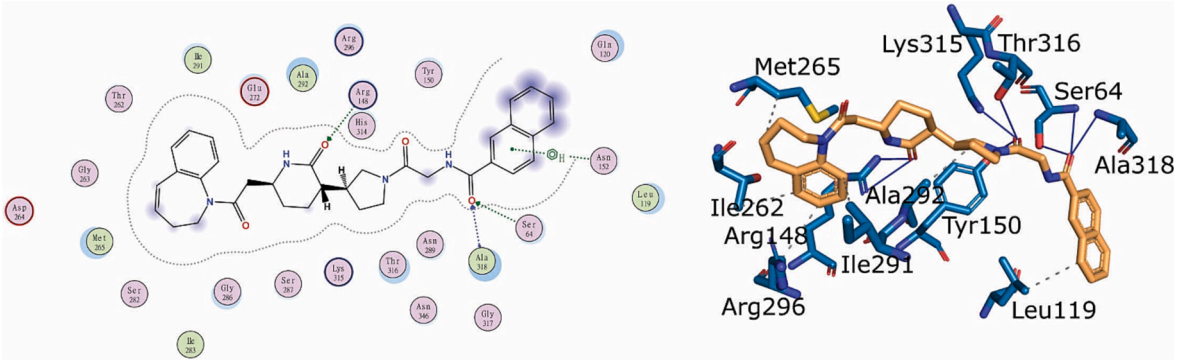

Fig. 4. Binding Interactions of S12 fragments complex with AmpC β-lactamase of *E. coli*. This complex shows good interactions pattern.

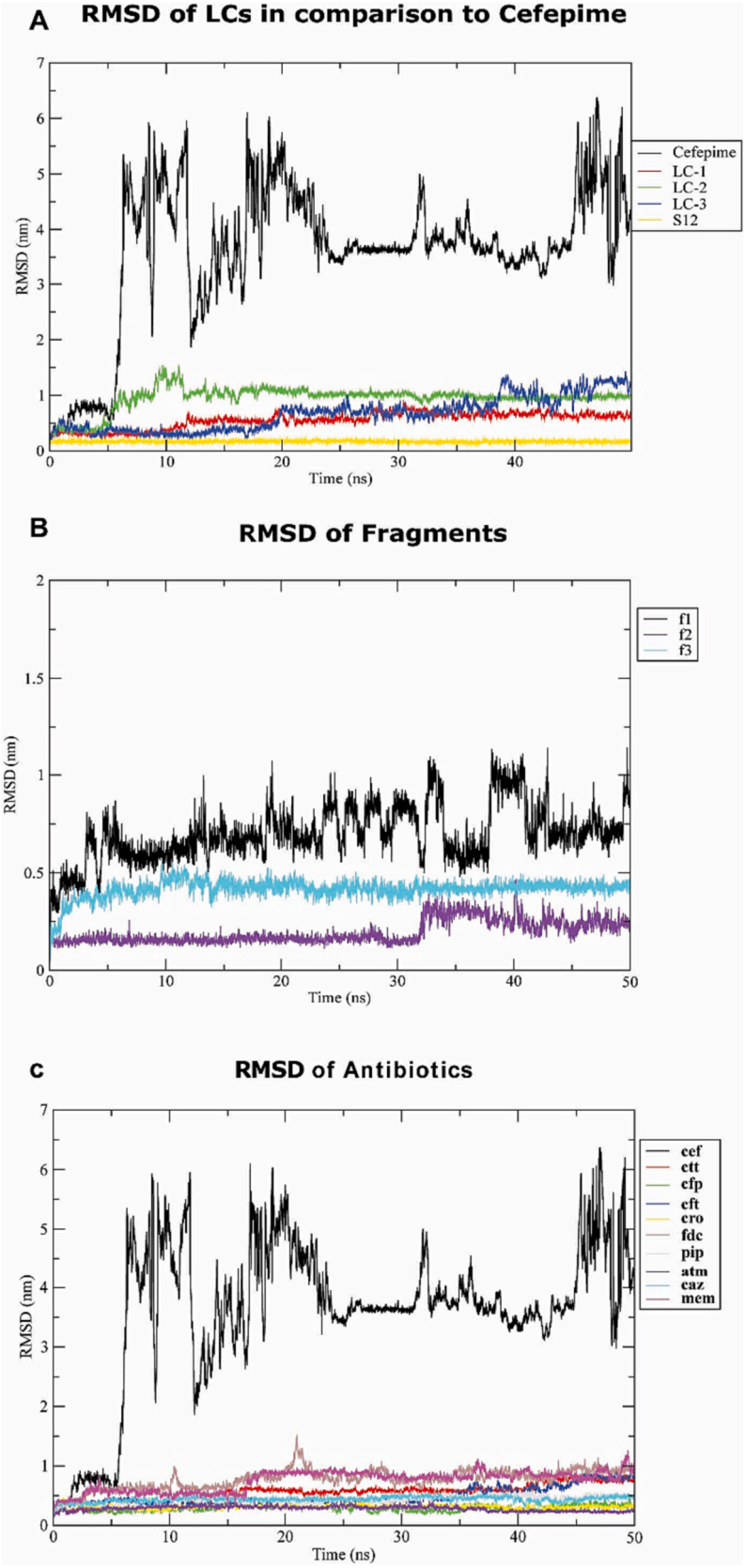

Fig. 5. Root Mean Square Deviation of all AmpC complexes during 50 ns MD Simulation: A: RMSD Plot of all LCs in comparison to Cefepime. Black: RMSD of Cef ligand Red: RMSD of LC-1 Green: RMSD of LC-2 Blue: RMSD of LC-3 Yellow: RMSD of S12 during 50 ns MD simulation. **B: RMSD Plot of individual fragments.** Black: RMSD of fragment f1 Cyan: RMSD of fragment f2 Violet: RMSD of fragment f3. **C: RMSD Plot of top ten antibiotic AmpC complexes during 50 ns MD Simulation.** cef: Cefepime ctt: Cefotetan cfp: cefoperazone cft: Ceftolozane cro: Ceftriaxone fdc: Cefiderocol pip: Piperacillin atm: Aztreonam caz: Ceftazidime mem: Meropenem.

displayed in (Fig. 6A). The plot depicted the amino acid residues on the x-axis whereas fluctuation values on the y-axis. It shows that only a few residues at the start fluctuated, but overall the structure was stable. Other fluctuations occurred from residues 200 to 230 in the loop region of the protein with a magnitude less than 0.4 nm, indicating stability. Moreover, active site region residues exhibited significant fluctuations peaks due to flexibility. RMSF plots of fragments and antibiotics also represent the same peaks as shown in (Fig. 6B) and (Fig. 6C). Overall, the pattern of fluctuations peaks by the residues shows that the ligands adapted well within the active site of the protein throughout the simulation process.

3.9.3. *Conformational changes of residues and their resultant flexibility*

The RMSD calculations depicted that the essential residues may remain stable throughout the simulation process as represented by averaged RMSF values for the protein backbone atoms as well as for complexes. The loop regions of protein remained more flexible in comparison to rest of secondary structure elements. The flexibility of protein with LCs was assessed by comparison of RMSF values as displayed in (Fig. 6). It disclosed higher flexibility in loop regions of the protein compared to the other secondary structural elements. The Residue regions 210–220, 240–250 and 310–320 represent loop region with higher RMSF values in case of all linked complexes and these residues also showed RMSF values within the acceptable ranges of maximum peak till 0.3 nm. This residual fluctuation pattern is predictive of the fact these fluctuations of loops cannot block entrance of active site and the active site remained open throughout simulation.

Throughout MD investigations, the flexibility of binding site residues was also evaluated to see whether the active site remained stable. The computed distances of different pocket residues using trajectories throughout different frames of simulation demonstrated that pocket remained wide throughout simulation process as shown in (Supplementary Figure S9). A deeper analysis of active site residues at different frames of simulation clearly indicated that binding pocket remained wide throughout different frames. The average distance between conserved residue Ser64 and Asn289 remained 1.12 nm ± 0.09 nm. Similarly, Lys67 is another important key interacting residue is away from Asn152 with an average distance of 0.48 nm ± 0.05 nm (Supplementary Figure S9 C). Also key residues Ser64 remains at an average distance of 1.58 nm ± 0.11 nm (Supplementary Figure S9 D). These distances illustrate flexibility of major residues in the pocket.

3.9.4. *Hydrogen bond analysis*

The Hydrogen bonds formed between protein and ligand are essential for maintaining a compact and proper conformation, in which residual associated flexibility play an integral role in ligand bond formation. The H bonds formed between the protein-ligands and their occupancies were calculated and depicted as a graph shown in (Fig. 7). Analysis of the generated plots indicated that LC-1 formed a total of twenty six hydrogen bonds contact points during the course of 50 ns MD simulations. The most frequent H-bond interactions include with the residues Arg204, Glu61 and Gly320. LC-2 formed thirty seven hydrogen bonds, most frequent being His210, Ser212 and Gly320. LC-3 formed thirty five hydrogen bonds including Ser212, Glu61, Asn289 and

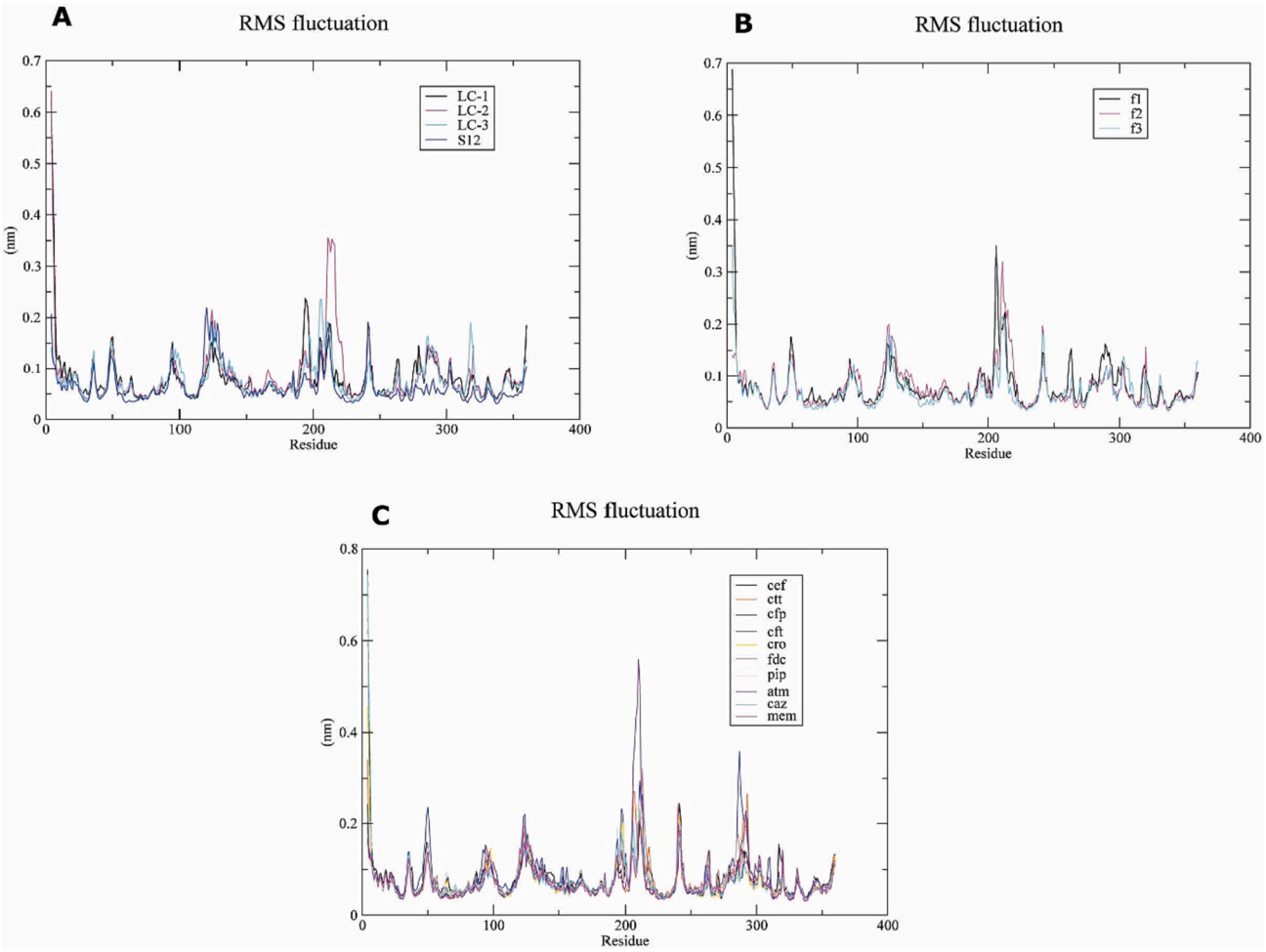

Fig. 6. Root Mean Square Fluctuations (RMSF) Analysis of all ligand-AmpC β-lactamase complexes throughout 50 ns MD simulation. A: RMSF Plot of LCs; **B:** RMSF Plot of fragments; **C:** RMSF Plot of Antibiotics.

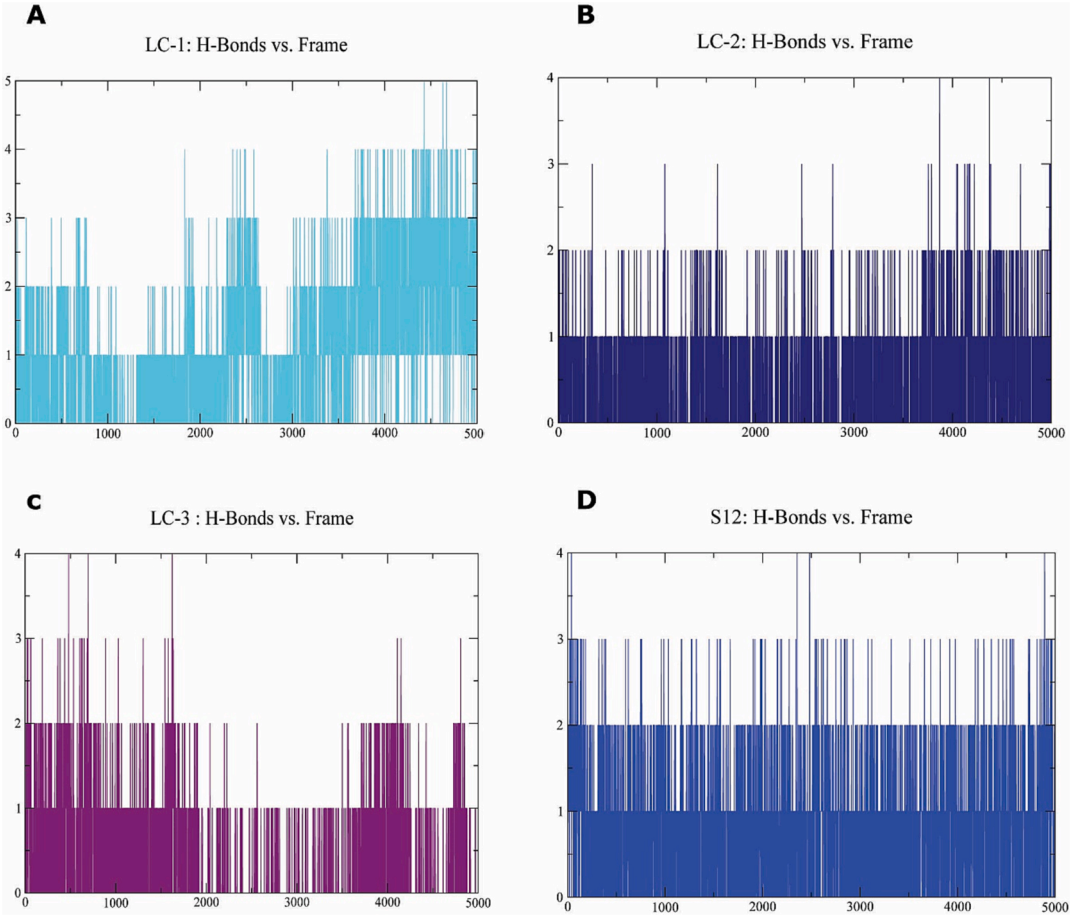

Fig. 7. Plot of Hydrogen bond formation during 50 ns MD simulation period of all four linked complexes. A: LC-1; **B:** LC-2; **C:** LC-3; **D:** S12. X axis shows different frames of simulations whereas Y axis shows H-bonds. LC-1, cyan color; LC-2, navy blue color; LC-3, purple color and S12, blue color.

Asn152. S12 formed nine stable hydrogen bonds with Ser64, Ala318, Arg148 and Tyr150. These bonds remain constant throughout the course of MD simulation (Table. S5). MD trajectories of fragments represented that the fragment f1 formed twenty eight H-bonds including residues with Ala292, Asn289 Arg148 most frequently during 50 ns MD studies. f2 formed eight H-bonds with Arg148 and Asn346 whereas f3 formed fourteen most frequent H-bonds with His314 and Tyr325 (Table. S6).

Similarly, all the antibiotics trajectories revealed number of H bonds with most common residues involved in bonding include Arg148, Asp264, Glu272, Arg296, Ala 318, Lys315 and Ser64 (Figure. S8 and Table. S7). Overall, these results provided evidence that LCs formed comparable H bonds with many standard antibiotics.

4. Discussion

The continuous incline of antibiotic resistance is a major public health problem of both developing and under-developed countries leading to failure of treatment options, higher management expenses, and increased mortality and morbidity (Aryal et al., 2020). Keeping in view of therapeutic aspect, pAmpC β-lactamases are becoming more significant and their identification is necessary for the surveillance along with epidemiological and infection control strategies (Saffar et al., 2016). The AmpC from *E. coli* has been chosen as a representative enzyme of class C β-lactamases (hydrolases, cephalosporinases). There are over 100 structures for this protein in the PDB, one of the wild type protein determined at 2.30 Å was selected [45]. The chromosomal along with plasmid encoded AmpC enzymes are continuously evolving in ways to hydrolyze broad-spectrum cephalosporin rings. AmpC β-lactamases of Gram negative bacteria especially *E. coli*, produce AmpC β-lactamases that are of particular importance.

Molecular docking is an essential primary screening method to identify important protein–ligand interactions of the complexes based on their affinity parameters (Bhardwaj et al., 2021). The docking analysis of nine thousand three hundred eighty eight fragments was performed against AmpC β-lactamase. The stability of all docked molecules was determined and were categorized by their total binding energy. The best three hundred thirty nine fragments were selected for further processing based on their good scores and interaction patterns. The most important amino acids involved in structural interactions of fragments and receptor were found to be Glu272, Lys315, Thr316, Met265, and Arg148 (Figure.S3). The formation of hydrogen bond plays a very essential role in the stability of protein–ligand complex. It is estimated that the drug with more hydrogen bond acceptors and hydrogen bond donors binds well with other molecules and possesses good solubility and absorption (Hubbard and Haider, 2010).

In this study, interactions of the four fragment-based linked molecules with AmpC β-lactamase were thoroughly explored by analysis of their binding patterns. It was observed that Ser212 amino acid of the protein was the key residue interacting with all of the lead compounds. The residues Ser212 and Gly320, depicted the fragment scaffolds linkage with previous boronic-acid based covalent inhibitors in earlier study (Morandi et al., 2008). These interactions resulted in 20-fold increased binding affinity of the said covalent inhibitor (Eidam et al., 2012, Nichols et al., 2014). Furthermore, the protein–ligand interaction pattern of these four top linked complexes show more interaction points with protein at 50 ns of MD simulation (Table.S4). The analysis of docked complexes revealed that the ligands were extensively bonded with the residues of the active site of AmpC β-lactamase with good

docking scores. All of the complexes as well as individual fragment revealed good binding interactions. Among all these LCs, S12 has shown maximum binding interactions including hydrogen bonding with Ser64, Arg148, Tyr150, Lys315, Thr316, Ala318 and hydrophobic interactions with Leu119, Thr262, Met265, Ile291, Ala292 and Arg296. The fragment based complex S12 showed exceptional number of interactions including hydrogen bonding with Arg148, Ser64 and Ala318 with maximum occupancies along with other amino acids after 50 ns MD simulation. These residues were also reported to influence the binding affinity of previous fragment inhibitors (Teotico et al., 2009).

To elucidate the conformational flexibility and stability of protein with the ligand molecules, LCs, fragments and best affinity antibiotics were allowed to undergo MD simulations for a time period of 50 ns. After completion of the simulation studies, resultant plots were generated using RMSD, RMSF and H bonds trajectories of all these protein complexes.

RMSD is one key factor to study a protein–ligand interaction. It computes average distance between the ligand atoms and targeted protein that helps in comparison of conformational changes along with the stability of protein in a dynamic state during simulation (Gupta et al., 2021). The RMSD values for the protein backbone C-α atoms in complex with the four LCs molecules were computed, and the resultant graph is depicted in (Fig. 5A). It was observed that the minimum and maximum RMSD values obtained by LC-1, LC-3 were of very low magnitude ranging from 0.2 nm to 0.8 nm. Among these complexes, S12 remained most stable and showed no fluctuation in RMSD values throughout 50 ns time period. This strongly demonstrates the conformational stability of the protein with respect to the ligands. The resultant plots depicted stable trajectories with smaller fluctuations showing that the protein backbone underwent slight structural changes. The analysis of trajectories also depicted a few major fluctuations during different time intervals but overall the structure was stabilized in the end. The individual fragments showed minimal fluctuations in RMSD values within the range of 0.2 to 0.8 nm indicating their overall stability.

The current regimen for UTIs treatment caused by AmpC β–lactamase producing *E. coli* include cephalosporins, nitrofurantion, fosfomycin, fluoroquinolones, cefepime, piperacillin-tazobactam and carbapenems (Bader et al., 2020). The best affinity antibiotics were screened against target protein and it was observed that aztreonam and ceftriaxone remained the most stable during 50 ns MD simulations Moreover, all the antibiotics showed minimum and maximum RMSDs in the range of 0.1–0.9 nm except for cefepime which showed fluctuations of high magnitude. All these findings were conclusive of the fact that linked complexes of cefepime remained stable conformation during the protein–ligand with only few conformational transitions in comparison with the conventional cefepime. Interestingly, it was also observed that number of interactions and contact points between the ligands and protein increased significantly after 50 ns simulations that is also indicative of stability of all these ligands within the protein pocket. The complexes remained stabilized within binding pocket by both polar and non-polar amino acid residues within 5 Å with the help of interections including hydrogen bonding, electrostatic and Van der Waal forces. The number of hydrogen bonds as well as hydrophobic interactions were reported to be more in number. To have an insight of the binding modes, frames were extracted at every 10 ns from the trajectories and rendered the LCs at the binding cavity which indicated that many residual contacts of LCs remained preserved throughout different frames of simulations (Table. S8) The RMSF values of all the ligands initially showed fluctuations of few residues and minor fluctuations of around residues from 200 and 230, which were less than 0.4 nm indicative of overall stability of the complexes within the target protein. The conducted MD simulation studies also revealed that hydrogen bonds have a substantial impact on the intermolecular recognition along with active center for the all protein complexes interaction as all the complexes exhibited significant number of hydrogen bond. It can be concluded that hydrogen bonds formed between complexes were comparable with the conventional antibiotics.

In the present study, the molecular docking guided virtual screening have identified some potential ligand complexes LC-1, LC-2, LC-3 and especially S12, as promising fragment inhibitors against AmpC β-lactamase. The interactions of the suggested potential candidates with the protein were analyzed for choosing the optimized complex. For further validation of molecular screening findings, MD simulations were performed that depicted the ligand-complex stability for the identified candidates. Certain fluctuations in the active site region residues were observed with significant peaks illustrating flexibility of protein for ligand binding. Moreover, computation of distances between active site residues and linked complexes (LCs) validated that LCs attained better stability compared to conventional cefepime that was displaced out of the frames of simulation. It can be concluded that all the designed fragment complexes indicated overall stable structural conformations with AmpC β-lactamase. This study provides an insight of fragment-based inhibitors with promising inhibition potential against AmpC β-lactamase of *E. coli* as compared to conventional antibacterials. It is acknowledged that computational studies have their limitations, and that further laboratory experimentation and clinical investigations are needed for the validation of the inhibitory effects as well as toxicity profiling of these candidates against AmpC β-lactamase of *E. coli* as potential drugs for *E. coli* infections.

5. Conclusion

The exploration of new molecules to inhibit the β-lactamase proteins remains a challenge to be solved in the clinical therapeutic field, especially in the context of bacterial resistance. The identification and discovery of new antibacterial agents has been substantially accelerated due to protein–ligand docking and molecular simulation approaches. In our study, using an in silico approach, we have proposed fragment-based linked complexes against AmpC β-lactamase of *E. coli*. When analysing dynamics stability, it was found that all complexes are stable due to presence of the RMSD values of all complexes in acceptable range. All these complexes showed improved behaviour than conventional cefepime antibiotic. S12 complex exhibited remarkable potential as antibacterial against AmpC β-lactamase of *E. coli*, as evident from higher binding affinity and stability compared to many other standard antibacterial drugs. The substantial inhibitory property of the compound was validated by the presence of conventional hydrogen bonds of complexes with the target protein. These findings concluded that current molecule has promising action and can serve as antibacterial agent. These potential compounds will further be elucidated in future wet lab experiments.

Declaration of Competing Interest

The authors declare that they have no known competing financial interests or personal relationships that could have appeared to influence the work reported in this paper.

Appendix A. Supplementary material

Supplementary data to this article can be found online at https://doi.org/10.1016/j.sjbs.2023.103884.

References

Aryal, S.C., Upreti, M.K., Sah, A.K., Ansari, M., Nepal, K., Dhungel, B., Adhikari, N., Lekhak, B., Rijal, K.R., 2020. Plasmid-mediated AmpC β-lactamase CITM and DHAM genes among gram-negative clinical isolates. Infect. Drug Resist. 4249–4261.

Bader, M.S., Loeb, M., Leto, D., Brooks, A.A., 2020. Treatment of urinary tract infections in the era of antimicrobial resistance and new antimicrobial agents. Postgrad. Med. 132, 234–250.

Bhardwaj, V.K., Singh, R., Das, P., Purohit, R., 2021. Evaluation of acridinedione analogs as potential SARS-CoV-2 main protease inhibitors and their comparison with repurposed anti-viral drugs. Comput. Biol. Med. 128, 104117.

Bischoff, S., Walter, T., Gerigk, M., Ebert, M., Vogelmann, R., 2018. Empiric antibiotic therapy in urinary tract infection in patients with risk factors for antibiotic resistance in a German emergency department. BMC Infect. Dis. 18, 1–7.
Black, J.A., Moland, E.S., Thomson, K.S., 2005. AmpC disk test for detection of plasmid-mediated AmpC β-lactamases in Enterobacteriaceae lacking chromosomal AmpC β-lactamases. J. Clin. Microbiol. 43, 3110–3113.
Bollag, G., Hirth, P., Tsai, J., Zhang, J., Ibrahim, P.N., Cho, H., Spevak, W., Zhang, C., Zhang, Y., Habets, G., 2010. Clinical efficacy of a RAF inhibitor needs broad target blockade in BRAF-mutant melanoma. Nature 467, 596–599.
Chilingaryan, Z., Yin, Z., Oakley, A.J., 2012. Fragment-based screening by protein crystallography: successes and pitfalls. Int. J. Mol. Sci. 13, 12857–12879.
Chilingaryan, Z., Headey, S.J., Lo, A.T., Xu, Z.-Q., Otting, G., Dixon, N.E., Scanlon, M.J., Oakley, A.J., 2018. Fragment-based discovery of inhibitors of the bacterial DnaG-SSB interaction. Antibiotics 7, 14.
Choudhury, C., 2021. Fragment tailoring strategy to design novel chemical entities as potential binders of novel corona virus main protease. J. Biomol. Struct. Dyn. 39, 3733–3746.
Da Silva, T.U., Pougy, K.D.C., Albuquerque, M.G., Da Silva Lima, C.H., Machado, S.D.P., 2022. Development of parameters compatible with the CHARMM36 force field for [Fe4S4] 2+ clusters and molecular dynamics simulations of adenosine-5'-phosphosulfate reductase in GROMACS 2019. J. Biomol. Struct. Dyn. 40, 3481–3491.
Eidam, O., Romagnoli, C., Dalmasso, G., Barelier, S., Caselli, E., Bonnet, R., Shoichet, B. K., Prati, F., 2012. Fragment-guided design of subnanomolar β-lactamase inhibitors active in vivo. Proc. Natl. Acad. Sci. 109, 17448–17453.
Ejaz, H., Zafar, A., Amin, H., 2014. Multidrug resistant AmpC β-lactamase producing Escherichia coli isolated from a paediatric hospital. Pak. J. Med. Sci. 30, 181.
Erlanson, D.A., Fesik, S.W., Hubbard, R.E., Jahnke, W., Jhoti, H., 2016. Twenty years on: the impact of fragments on drug discovery. Nat. Rev. Drug Discov. 15, 605–619.
Fisher, J.F., Meroueh, S.O., Mobashery, S., 2005. Bacterial resistance to β-lactam antibiotics: compelling opportunism, compelling opportunity. Chem. Rev. 105, 395–424.
Friedman, N.D., Temkin, E., Carmeli, Y., 2016. The negative impact of antibiotic resistance. Clin. Microbiol. Infect. 22, 416–422.
Gales, A. C., Jones, R. N., Gordon, K. A., Sader, H. S., Wilke, W. W., Beach, M. L., Pfaller, M. A., Doern, G. V. & Sentry Study Group Latin America, T. 2000. Activity and spectrum of 22 antimicrobial agents tested against urinary tract infection pathogens in hospitalized patients in Latin America: report from the second year of the SENTRY antimicrobial surveillance program (1998). J. Antimicrob. Chemother. 45, 295-303.
Ghosh, B., Mukherjee, M., 2016. Emergence of co-production of plasmid-mediated AmpC beta-lactamase and ESBL in cefoxitin-resistant uropathogenic Escherichia coli. Eur. J. Clin. Microbiol. Infect. Dis. 35, 1449–1454.
Gupta, S., Singh, A.K., Kushwaha, P.P., Prajapati, K.S., Shuaib, M., Senapati, S., Kumar, S., 2021. Identification of potential natural inhibitors of SARS-CoV2 main protease by molecular docking and simulation studies. J. Biomol. Struct. Dyn. 39, 4334–4345.
Haenni, M., Chatre, P., Madec, J.-Y., 2014. Emergence of Escherichia coli producing extended-spectrum AmpC β-lactamases (ESAC) in animals. Front. Microbiol. 5, 53.
Hollingsworth, S.A., Dror, R.O., 2018. Molecular dynamics simulation for all. Neuron 99, 1129–1143.
Hubbard, R. E. & Haider, M. K. 2010. Hydrogen bonds in proteins: role and strength. *eLS*.
Humphrey, W., Dalke, A., Schulten, K., 1996. VMD: visual molecular dynamics. J. Mol. Graph. 14, 33–38.
Izadi, S., Anandakrishnan, R., Onufriev, A.V., 2014. Building water models: a different approach. J. Phys. Chem. Lett. 5, 3863–3871.
Jacoby, G.A., 2009. AmpC β-lactamases. Clin. Microbiol. Rev. 22, 161–182.
Karam, M.R.A., Habibi, M., Bouzari, S., 2019. Urinary tract infection: Pathogenicity, antibiotic resistance and development of effective vaccines against Uropathogenic Escherichia coli. Mol. Immunol. 108, 56–67.
Karplus, M., Petsko, G.A., 1990. Molecular dynamics simulations in biology. Nature 347, 631–639.
Konteatis, Z., 2021. What makes a good fragment in fragment-based drug discovery? Expert Opin. Drug Discov. 16, 723–726.
León-Buitimea, A., Morones-Ramírez, J.R., Yang, J.H., Peña-Miller, R., 2021. Facing the Upcoming of Multidrug-Resistant and Extensively Drug-Resistant Bacteria. Novel Antimicrobial Therapies (NATs). Frontiers Media SA.
Li, Q., 2020. Application of fragment-based drug discovery to versatile targets. Front. Mol. Biosci. 7, 180.
Lima, L.M., Da Silva, B.N.M., Barbosa, G., Barreiro, E.J., 2020. β-lactam antibiotics: An overview from a medicinal chemistry perspective. Eur. J. Med. Chem. 208, 112829.
Mann, R., Mediati, D. G., Duggin, I. G., Harry, E. J. & Bottomley, A. L. 2017. Metabolic adaptations of uropathogenic E. coli in the urinary tract. Front. Cell. Infect. Microbiol., 7, 241.
Martínez-Rosell, G., Giorgino, T., De Fabritiis, G., 2017. PlayMolecule ProteinPrepare: a web application for protein preparation for molecular dynamics simulations. J. Chem. Inf. Model. 57, 1511–1516.
Mondal, M., Radeva, N., Fanlo-Virgós, H., Otto, S., Klebe, G., Hirsch, A.K., 2016. Fragment linking and optimization of inhibitors of the aspartic protease endothiapepsin: fragment-based drug design facilitated by dynamic combinatorial chemistry. Angew. Chem. Int. Ed. 55, 9422–9426.
Morandi, S., Morandi, F., Caselli, E., Shoichet, B.K., Prati, F., 2008. Structure-based optimization of cephalothin-analogue boronic acids as β-lactamase inhibitors. Bioorg. Med. Chem. 16, 1195–1205.
Murray, C.W., Newell, D.R., Angibaud, P., 2019. A successful collaboration between academia, biotech and pharma led to discovery of erdafitinib, a selective FGFR inhibitor recently approved by the FDA. MedChemComm 10, 1509–1511.
Nichols, D.A., Renslo, A.R., Chen, Y., 2014. Fragment-based inhibitor discovery against β-lactamase. Future Med. Chem. 6, 413–427.
O'neill, J. 2014. Review on antimicrobial resistance. *Antimicrobial resistance: tackling a crisis for the health and wealth of nations,* 2014.
Pfeifer, Y., Cullik, A., Witte, W., 2010. Resistance to cephalosporins and carbapenems in Gram-negative bacterial pathogens. Int. J. Med. Microbiol. 300, 371–379.
Pitout, J.D., 2012. Extraintestinal pathogenic Escherichia coli: an update on antimicrobial resistance, laboratory diagnosis and treatment. Expert Rev. Anti Infect. Ther. 10, 1165–1176.
Rezatofighi, S.E., Mirzarazi, M., Salehi, M., 2021. Virulence genes and phylogenetic groups of uropathogenic Escherichia coli isolates from patients with urinary tract infection and uninfected control subjects: a case-control study. BMC Infect. Dis. 21, 1–11.
Ross, G.A., Rustenburg, A.S., Grinaway, P.B., Fass, J., Chodera, J.D., 2018. Biomolecular simulations under realistic macroscopic salt conditions. J. Phys. Chem. B 122, 5466–5486.
Saffar, H., Niaraki, N.A., Tali, A.G., Baseri, Z., Abdollahi, A., Yalfani, R., 2016. Prevalence of AmpC β-lactamase in clinical isolates of Escherichia coli, Klebsiella spp., and Proteus mirabilis in a Tertiary Hospital in Tehran, Iran. *Jundishapur.* J. Microbiol. 9.
Samra, R.M., Soliman, A.F., Zaki, A.A., Ashour, A., Al-Karmalawy, A.A., Hassan, M.A., Zaghloul, A.M., 2021. Bioassay-guided isolation of a new cytotoxic ceramide from Cyperus rotundus L. S. Afr. J. Bot. 139, 210–216.
Shrestha, P., Cooper, B. S., Coast, J., Oppong, R., Do Thi Thuy, N., Phodha, T., Celhay, O., Guerin, P. J., Wertheim, H. & Lubell, Y. 2018. Enumerating the economic cost of antimicrobial resistance per antibiotic consumed to inform the evaluation of interventions affecting their use. *Antimicrobial Resistance & Infection Control,* 7, 1-9.
Spyrakis, F., Santucci, M., Maso, L., Cross, S., Gianquinto, E., Sannio, F., Verdirosa, F., De Luca, F., Docquier, J.-D., Cendron, L., 2020. Virtual screening identifies broad-spectrum β-lactamase inhibitors with activity on clinically relevant serine-and metallo-carbapenemases. Sci. Rep. 10, 12763.
Swaminathan, B., Barrett, T.J., Hunter, S.B., Tauxe, R.V., Force, C.P.T., 2001. PulseNet: the molecular subtyping network for foodborne bacterial disease surveillance, United States. Emerging Infectious Diseases 7, 382.
Tan, C.W., Chlebicki, M.P., 2016. Urinary tract infections in adults. Singapore Med. J. 57, 485.
Teotico, D.G., Babaoglu, K., Rocklin, G.J., Ferreira, R.S., Giannetti, A.M., Shoichet, B.K., 2009. Docking for fragment inhibitors of AmpC β-lactamase. Proc. Natl. Acad. Sci. 106, 7455–7460.
Usher, K.C., Blaszczak, L.C., Weston, G.S., Shoichet, B.K., Remington, S.J., 1998. Three-Dimensional Structure of AmpC β-Lactamase from Escherichia c oli Bound to a Transition-State Analogue: Possible Implications for the Oxyanion Hypothesis and for Inhibitor Design. Biochemistry 37, 16082–16092.
Vaidya, A., Jain, S., 2017. Chemistry and Pharmacology of β-Lactam Analogs. Apple Academic Press, Handbook of Research on Medicinal Chemistry.
Vanommeslaeghe, K., Hatcher, E., Acharya, C., Kundu, S., Zhong, S., Shim, J., Darian, E., Guvench, O., Lopes, P., Vorobyov, I., 2010. CHARMM general force field: A force field for drug-like molecules compatible with the CHARMM all-atom additive biological force fields. J. Comput. Chem. 31, 671–690.
Vilar, S., Cozza, G., Moro, S., 2008. Medicinal chemistry and the molecular operating environment (MOE): application of QSAR and molecular docking to drug discovery. Curr. Top. Med. Chem. 8, 1555–1572.
Volkamer, A., Kuhn, D., Rippmann, F., Rarey, M., 2012. DoGSiteScorer: a web server for automatic binding site prediction, analysis and druggability assessment. Bioinformatics 28, 2074–2075.
Wedberg, R., Abildskov, J., Peters, G.N.H., 2012. Protein dynamics in organic media at varying water activity studied by molecular dynamics simulation. J. Phys. Chem. B 116, 2575–2585.
Weiner, L. M., Webb, A. K., Limbago, B., Dudeck, M. A., Patel, J., Kallen, A. J., Edwards, J. R. & Sievert, D. M. 2016. Antimicrobial-resistant pathogens associated with healthcare-associated infections: summary of data reported to the National Healthcare Safety Network at the Centers for Disease Control and Prevention, 2011–2014. *infection control & hospital epidemiology,* 37, 1288-1301.
Yu, H.S., Modugula, K., Ichihara, O., Kramschuster, K., Keng, S., Abel, R., Wang, L., 2020. General theory of fragment linking in molecular design: why fragment linking rarely succeeds and how to improve outcomes. J. Chem. Theory Comput. 17, 450–462.